Water at nanoscale confined in single-walled carbon nanotubes studied by NMR

EUROPHYSICS LETTERS 1 March 2004

Europhys. Lett., **65** (5), pp. 678–684 (2004)
DOI: 10.1209/epl/i2003-10160-9

Water at nanoscale confined in single-walled carbon nanotubes studied by NMR

S. Ghosh[1], K. V. Ramanathan[2] and A. K. Sood[1]

[1] *Department of Physics, Indian Institute of Science - Bangalore 560 012, India*
[2] *Sophisticated Instruments Facility, Indian Institute of Science Bangalore 560 012, India*

(received 18 September 2003; accepted in final form 11 December 2003)

PACS. 61.46.+w – Nanoscale materials: clusters, nanoparticles, nanotubes, and nanocrystals.
PACS. 87.64.Hd – EPR and NMR spectroscopy.
PACS. 82.60.Nh – Thermodynamics of nucleation.

Abstract. – Proton NMR studies have been carried out as a function of temperature from 210 K to 300 K on water confined within single-walled carbon nanotubes. The NMR lineshape at and below the freezing point of bulk water is asymmetric and can be decomposed into a sum of two Lorentzians. The intensities of both the components decrease with the lowering of the temperature below 273 K, one component, L_1, vanishing below 242 K and the other component, L_2, below 217 K. Following the simulations of Koga *et al.* showing that the radial density profile of confined water in single-wall carbon nanotubes has a distribution peak at the center which disappears below the freezing temperature, the L_1-component is associated with the protons of the water molecules at the center and the L_2-component is associated with protons of water molecules at a distance of ~ 3 Å from the walls of the nanotubes. In this scenario the complete freezing of the water at ~ 212 K is preceded by the withdrawal of the water molecules from the center.

Carbon nanotubes are unique in many ways not only for their unusual electric and mechanical properties resulting in many potential applications [1–4] but also for their quasi–one-dimensional nanometric-sized hollow structures. Single-walled carbon nanotubes (SWNT) assemble themselves into a two-dimensional triangular lattice to form bundles of aligned nanotubes with a nearest intertubular gap of ~ 0.3 nm [5]. Thus, the inside of the nanotubes and the interstitial gaps in the bundle provide very well characterized nanometer-sized volumes to show how liquids, in particular, water, behave on nanoscale [6, 7]. These studies on confined water may also have relevance to understand the behavior of water on nanoscale in biological environments like in ion channels [8].

SWNT can be wetted by liquids with surface tension less than 0.2 N/m and hence water (surface tension ~ 0.07 N/m) is expected to wet nanotubes [9]. Recent computer simulations have brought out many new features in the behavior of water inside carbon nanotubes [6, 10–12]. It is shown that water inside cylindrical pores of SWNT of diameter ($2R$) of 1.42 nm is expected to show a first-order freezing (melting) transitions at about 230 K (260 K). The low-temperature phase is an ice-nanotube composed of orderly stacked 6- or 7-membered water rings. The simulations [6] have also shown a significant change in the radial density

distribution within the nanotubes as temperature is lowered. The interesting behavior of water under confinement is related to the disruption of the hydrogen-bond network between water molecules, depending on the hydrophobic or hydrophilic nature of the confining surface. The average number of hydrogen bonds is reduced within the nanotubes relative to four in bulk water. This results in the depression of the freezing (melting) transition temperature of water. It is observed in the simulations [11, 12] that the average number of hydrogen bonds for water inside the tube has a maximum between the center and the walls of the nanotubes. Molecular-dynamics simulations have also shown that it is energetically unfavorable for the water molecules to stay in the hydrophobic van der Waals gaps between the nanotubes in a bundle [13]. First-principle calculations [14] predict that the water molecules should be at a distance of 0.27 nm from the surface of the nanotubes. Recent X-ray diffraction (XRD) measurements [15] of water confined inside SWNT with average diameter $\sim$ 1.37 nm have been analyzed by comparing the data with the simulated XRD patterns using three different models for the radial density distribution of water inside the tubes [12]. The analysis revealed that the liquid-like water is transformed into ice nanotubes at 235 K, similar to the simulation results of Koga *et al.* [6]. It may be kept in mind that the simulations were performed under axial pressures ranging from 50 to 500 Mpa and the transition temperatures ranged from 200 to 300 K depending on the tube diameters.

In this paper we report proton nuclear magnetic resonance (NMR) studies of water confined inside SWNT in the temperature range of 300 to 200 K. NMR has a unique advantage in studying freezing phenomena of confined water. This is because the transverse (spin-spin) relaxation time, T_2, of water is much larger ($\sim$ a few seconds) than that of solid ice ($\sim 6\,\mu$s). This will ensure that the NMR signal below 273 K (the freezing temperature of bulk water) will arise essentially from the non-frozen confined water in the sample. NMR studies have been carried out on the freezing phenomena of water confined in pores of silica gel, controlled pore glass, zeolites etc. [16–19]. The lowering of the freezing point has been verified for many adsorbents and adsorbates. The suppression, ΔT, of the freezing temperature is related to the pore radius R and to the thermodynamic properties of the liquid by the Gibbs-Thompson equation [20]: $\Delta T = -k/R = -2\gamma M T_0/(R\rho\Delta H)$, where T_0 is the normal freezing point of the bulk liquid, ΔH the molar heat, γ the surface tension, M the molecular weight and ρ the density of the liquid. For water in silica gel and zeolites [21], k has been determined to be $\sim 5 \times 10^{-8}$ K/m, which will imply a freezing temperature of 203 K for $R = 0.7$ nm. For larger diameter pores ($\sim$ 6.2 to 7.4 nm), it has been seen that the water layer near the walls of the pores freezes at a much lower temperature than predicted by the Gibbs-Thompson equation [16]. In this paper, we show a novel result that the freezing of water inside single-wall carbon nanotubes occurs in two steps; and the complete freezing occurs at a temperature of $\sim$ 212 K.

NMR measurements were carried out on a 300 MHz Bruker DSX-300 FT-NMR spectrometer using a wide-line probe. The proton ^{1}H NMR spectra were acquired with a $\pi/2$ pulse length of 4 μs with recycle delay time of 10 s and 1000 transients were accumulated. The temperature variation was achieved using a Bruker BVT2000 temperature controller with a temperature stability better than ± 1 K. SWNT assembled in bundles were prepared by the arc discharge method followed by an extensive purification process described earlier [22, 23]. The acid treatment also results in opening of the nanotubes. The average diameter of the tubes was 1.4 nm as determined from the Raman scattering of the radial breathing mode of the nanotubes [3]. The sample of SWNT ($\sim$ 2.5 mg) was completely soaked with double-distilled low-conductivity water in a quartz tube which was kept at the center of the detection coil. The temperature of the sample was lowered from room temperature to 200 K and the NMR spectra were recorded in the heating run. An equilibrium time of 30 minutes was allowed at each temperature before collecting data.

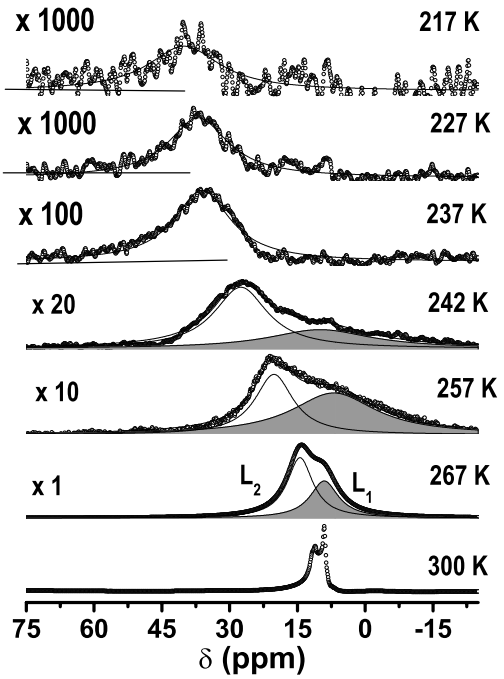

Fig. 1

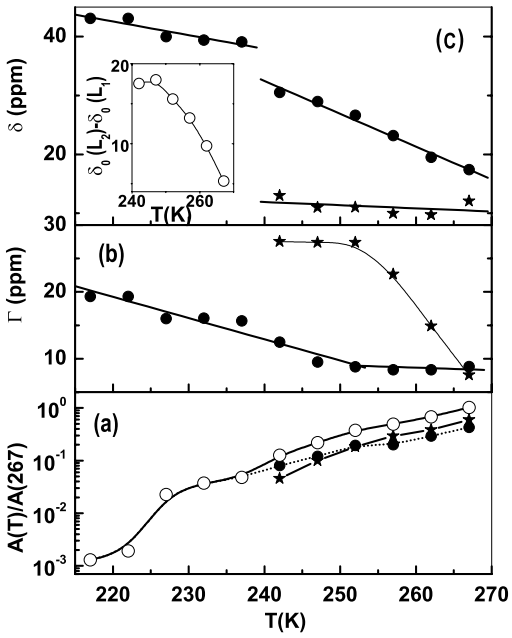

Fig. 2

Fig. 1 – Temperature dependence of the proton NMR spectra (open circles). The multiplicative intensity scale factors and the corresponding temperatures are given by the left side of the spectrum. The two component Lorentzian fits, L_1 (shaded) and L_2, are shown by solid lines.

Fig. 2 – (a) Temperature dependence of the normalized total area (A) under the entire spectra (open circles), area of the L_1 (filled stars) and of the L_2 (filled circles) component. All the areas are normalized with respect to the total integrated area at 267 K. (b) Full width at half-maximum (Γ) of the L_1 (filled stars) and L_2 (filled circles) component. (c) Temperature dependence of the peak positions of the L_1 (filled stars) and L_2 (filled circles) component. The inset of the figure shows the relative change in the peak positions.

Figure 1 shows the ^{1}H NMR spectra at a few typical temperatures. The intensity scale factors are given at the left side of the spectra, except for the spectra at 300 K, *i.e.* before the onset of freezing of bulk water when the intensity is higher by several orders. The spectrum at 300 K shows a narrow peak at a chemical shift (δ) of 12.06 ppm and a broader peak at 13.8 ppm (note that 1 ppm = 300 Hz). This may be compared with the NMR spectra of bulk water which gives a motionally narrowed peak at 4.6 ppm. We attribute the narrow peak at 12.06 ppm to the excess free water present in the SWNT. The additional downfield shift possibly arises from the presence of the SWNT having a large negative molar magnetic susceptibility ($\sim -10^{-5}\,\mathrm{cm}^3/\mathrm{mole}$) [24]. Below 273 K, the free water in the sample freezes and hence the signal obtained is only from the mobile water in the cylindrical pores of the nanotubes. As temperature is lowered, the intensity of the spectrum decreases and the spectrum at 217 K is barely observable. The low-temperature spectra between 242–267 K reveal an asymmetric lineshape. In the case of benzene adsorbed in porous silica an asymmetric lineshape has been reported [18], which has been attributed to the pore size distribution. An average chemical shift was also calculated which was related to the mean diameter of the pores. In the present

case, the variation in the diameter of SWNT [3] is known to be less than 5% which would not lead to an observable asymmetry. Considering the high magnetic susceptibility effects expected in SWNT and the reported simulations on the state of water inside the nanotubes [6], we consider an alternative explanation.

The asymmetric lineshape of the spectra obtained between 267 K and 242 K can be fitted to a sum of two Lorentzians (L_1 and L_2) as shown in fig. 1. It can be seen that the component L_1 broadens as temperature is lowered and disappears in the spectrum recorded at 237 K. Below 237 K only the L_2-component survives and the spectra is symmetric. The component L_2 also disappears below 217 K, the temperature at which the entire signal becomes indistinguishable from the background. Thus one can see that the freezing occurs in two steps. Figures 2 show the variations of the integrated intensity (A), full width at half-maximum (Γ) and peak position (δ_0) as a function of temperature obtained by Lorentzian fitting of the data. All the areas are normalized with respect to the total integrated area at 267 K. Figure 2(a) shows the variation of the normalized total area under the entire spectra (open circles), the area of the L_1-component (filled stars), the area of the L_2-component (filled circles). The area of component L_1 is larger than that of L_2 above 252 K, below which the situation is reversed. Figure 2(b) shows the FWHM (Γ) variation of the two Lorentzian components L_1 (filled stars), L_2 (filled circles). With a decrease of temperature, $\Gamma(L_1)$ shows a rapid increase before saturating to the value of ~ 8.2 kHz at 252 K. However, $\Gamma(L_2)$ does not vary much for temperatures greater than 252 K, below which it increases. The increase in the value of Γ is indicative of the fact that the water molecules have progressively lower mobility due to confinement. Figure 2(c) shows the position of the peak maximum (δ_0) of the two components L_1 and L_2 with the lowering of the temperature. The variation of $\delta_0(L_1)$ with temperature is small with $\delta_0(L_1)/\Delta T = 0.05$ ppm/K. However, $\delta_0(L_2)$ shows a linear downfield increase with temperature with a distinct jump ($\Delta\delta(\text{ppm})/\delta(242) = 0.3$) at 237 K. The slopes $\delta_0(L_2)/\Delta T = 0.55$ ppm/K for temperatures greater than 242 K and 0.23 ppm/K for temperatures below 242 K. The jump in the $\delta_0(L_2)$ also coincides with the loss of the L_1-component. The inset of fig. 2(c) shows the variation of $\delta_0(L_2) - \delta_0(L_1)$ in the temperature range between 267 K and 242 K. The difference in the peak position increases almost linearly. The peak position of L_2 shows a very large variation with $[\{\delta_0(267) - \delta_0(217)\}/\delta_0(267\,\text{K})] = -1.48$ in the temperature range from 267 K to 217 K. This downfield shift of the peak position can arise, in principle, from i) increase in the density (ρ) of water given [25] by $\Delta\delta/\delta = 2.03\Delta\rho/\rho$, where δ is in ppm and ρ is in gm/cm^3, ii) change in the magnetic susceptibility of nanotubes (χ_{NT}). However, the reported change in the parameters ρ [6] and χ_{NT} [26] is not sufficient([1]) to account for the large variation in the peak position of L_2.

Before we present a model to understand our NMR data based on the simulation results on the state of water inside the tubes, we rule out the possibility of contributions to NMR spectra (below 273 K) from water molecules adsorbed on the outside of the nanotube bundles. Even though the nanotube surface is corrugated, the structural properties of water at the nanotube-water interface are similar to those seen for water at an idealized graphite surface [27]. The enthalpies of water immersion of singe-walled carbon nanotube horns showed a very weak interaction between the water molecules and the hydrophobic carbon nanotubular structure [28]. Since our NMR experiments on water adsorbed on graphite did not show any measurable suppression of the freezing/melting temperature of water, we rule out the contributions of the adsorbed water on the nanotube surface to the NMR spectra below 273 K.

([1])It is reported that $\Delta\chi_{\text{NT}}/\chi_{\text{NT}}(267\,\text{K}) = 0.13(\Delta\chi_{\text{NT}} = \chi_{\text{NT}}(267) - \Delta\chi_{\text{NT}}(217))$ [26] in the temperature range from 267 K to 217 K. Besides the change in χ_{NT} would influence both the peaks L_1 and L_2 by the same amount. The experimental results, however, show that $\delta_0(L_2)$ has a much larger temperature variation than $\delta_0(L_1)$.

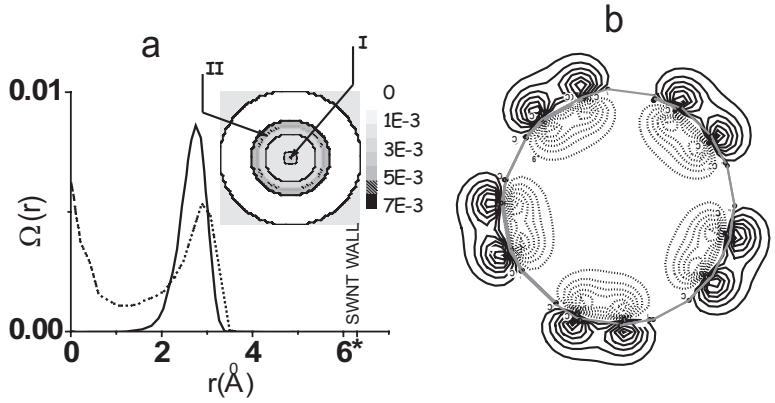

Fig. 3 – (a) The radial density profile [6] of water molecules in a tube of diameter 12.5 Å at 320 K (dotted line) and 245 K (solid line). The inset shows the mesh plot of the above radial density profile showing the regions I and II. (b) Bonding (solid line) and antibonding (dotted line) π band orbitals obtained by *ab initio* quantum chemical cluster calculations.

Accordingly, we attribute the observation of two broad bands in NMR spectra below 267 K (cf. fig. 1) to the presence of two components of confined water. Figure 3(a) shows the radial density distribution [6] $\Omega(r)$ of water confined inside SWNT of radius 6.3 Å at 320 K which is above the freezing temperature (dotted line) and at 240 K which is below the freezing temperature (solid line). The $\Omega(r)$ at 320 K shows two prominent features, one at the center (region I of the inset of fig. 3(a)) and the other 3 Å away from the wall (region II of the inset of fig. 3(a)). Most remarkably, the peak in $\Omega(r)$ at $r = 0$ is absent at 240 K, *i.e.* when freezing occurs, with the lowering of the temperature, the mobile water molecules move from region I to region II. This causes an increase of the density of water in region II coinciding with the jump in chemical shift observed for line L_2. An increase in the density [10] $\Delta\rho/\rho = 0.12$ on freezing has also been predicted by computer simulations [10], hence [25] $\Delta\delta/\delta = 0.24$. We assign the L_1-component to the water molecules in region I and L_2 to the water molecules in region II. It is

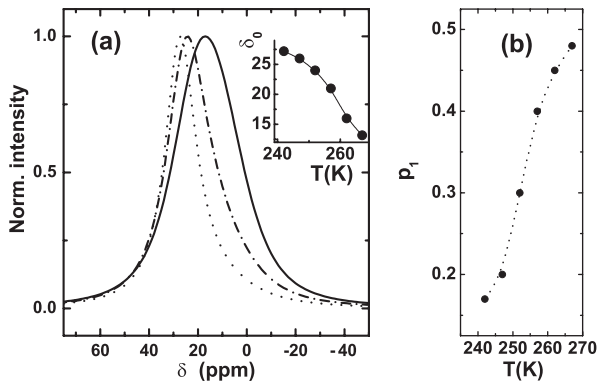

Fig. 4 – (a) Simulated NMR lineshapes at few selected temperatures (solid line (267 K), dash-dotted line (252 K), dotted line (242 K)). The inset shows the temperature variation of the peak positions of the simulated spectra. (b) Temperature dependence of the occupancy probability p_1.

to be noted that even at 267 K, $\delta_0(L_2) - \delta_0(L_1) = 5.3$ ppm (cf. fig. 2(c), inset). We offer a plausible explanation and justify the assignment of the lower shielded L_2-component to the water molecules in the region II, *i.e.* near the walls. Figure 3(b) shows the bonding (solid line) and antibonding (dotted line) π-orbitals of the nanotubes obtained [29] by *ab initio* quantum chemical calculations using the GAMESS package [30]. It can be seen that the bonding π-orbitals have a preference to lie outside the tube, whereas their antibonding counterparts lie inside it. This causes the inner side of the nanotubes to behave like an acceptor [31]. The presence of the acceptor-like walls of the nanotubes will result in the redistribution of the electronic charge in the water molecules near the wall (region II) by drawing the electrons away, thus causing a reduction in the electron density around the protons. This would result in a reduction of the shielding constant (σ) causing a downfield chemical shift. However, this effect would be significantly less for water molecules at the center. The large downfield shift of the peak position in the temperature range from 267 to 242 K of the L_2-component can be understood within the framework of the "two-level jump process" [32]. In this model the water molecules in the region I and II characterized by their resonance frequencies δ_1 and δ_2 ($\delta_1 - \delta_2 = 30$ ppm) and occupation probabilities p_1 and p_2 ($p_2 = 1 - p_1$) exchange positions with a jump rate λ. Figure 4(a) shows the simulated NMR spectra [32,33] for various temperatures using $\lambda = 7.5$ kHz (*i.e.* 25 ppm) and p_1 as the only adjustable parameter shown in fig. 4(b). The inset of fig. 4(a) shows the shift in the peak maxima of the simulated spectra as a function of temperature which agrees remarkably well with the experimentally observed variation (cf. fig. 2(c)). Since λ (25 ppm) is of the order of the peak separation, the spectrum obtained shows signatures of relaxation as well as resonance phenomenon. The large variation in the peak position of L_2 before freezing occurs at 242 K and can thus be attributable to this dynamic process.

To summarize, our NMR data suggest that a change in the density distribution of water molecules occurs and the center is depleted of the water molecules below 242 K. Below this temperature, the fraction of mobile water molecules decrease and the complete freezing occurs at ~ 212 K. It would be very interesting to do careful simulations to look at the pre-transition redistribution of water molecules inside the nanotube. More NMR experiments are desirable on other liquids like benzene and cyclohexane in carbon nanotubes of different diameters to understand the dynamics of liquids at nanoscale.

* * *

We thank Prof. A. Kumar for very stimulating discussions. AKS thanks the Department of Science and Technology (Government of India) for continued support of his research and Prof. C. N. R. Rao for his interest in these studies. We gratefully thank Prof. C. N. R. Rao and Dr. A. Govindaraj for the SWNT samples.

REFERENCES

[1] Ghosh S., Sood A. K. and Kumar N., *Science*, **299** (2003) 1042.
[2] Baughman R. H. *et al.*, *Science*, **284** (1999) 1340.
[3] Ghosh S., Sood A. K. and Rao C. N. R., *J. Appl. Phys.*, **92** (2002) 1165.
[4] Rao C. N. R., Satishkumar B. C., Govindraj A. and Manasi Nath, *Chem. Phys. Chem.*, **2** (2001) 78.
[5] Dresselhaus M. S., Dresselhaus G. and Eklund P. C., *Science of Fullerenes and Carbon Nanotubes* (Academic Press, New York) 1996, Chapt. 19.
[6] Koga K., Gao G. T., Tanaka H. and Zeng X. C., *Nature*, **412** (2001) 802.
[7] Hummer G., Rasaiah J. C. and Noworyta J. P., *Nature*, **414** (2001) 188.

[8] Sanson M. S. P. and Biggin P. C., *Nature*, **414** (2001) 156.
[9] Dujardin E., Ebbesen T. W., Hiura H. and Tanigaki K., *Science*, **265** (1994) 1850.
[10] Koga K., Gaob G. T., Tanakac H. and Zeng X. C., *Physica A*, **314** (2002) 462.
[11] Marti J. and Gordillo M. C., *Phys. Rev. E*, **64** (2001) 021504.
[12] Gordillo M. C. and Martí J., *Chem. Phys. Lett.*, **329** (2000) 341.
[13] Werder T., Walther J. H. and Koumoutsakos P., *Technical Proceedings of the Second International Conference on Computational Nanoscience and Nanotechnology-ICCN 2002*, 2002, p. 490.
[14] Zhao J., Buldum A., Han J. and Lu J. P., *Nanotechnology*, **13** (2002) 195.
[15] Maniwa Y., Kataura H., Abe M., Suzuki S., Achiba Y., Kira H. and Matsuda K., *J. Phys. Soc. Jpn.*, **71** (2002) 2863.
[16] Ayyappan S., Suryaprakash N., Ramanathan K. V. and Rao C. N. R., *J. Porous Mater.*, **6** (1999) 5.
[17] Strange J. H. and Rahman M., *Phys. Rev. Lett.*, **71** (1993) 3589.
[18] Hansen W. W., Scmidt R. and Stocker M., *J. Phys. Chem.*, **100** (1996) 11396.
[19] Akenes D. W. and Kimtys L., *Appl. Magn. Reson.*, **23** (2002) 51.
[20] Jackson C. L. and McKenna G. B., *J. Chem. Phys.*, **93** (1990) 9002.
[21] Hansen E. W., Stocker M. and Schmidt R., *J. Phys. Chem.*, **100** (1996) 2195.
[22] Teredesai P. V., Sood A. K., Muthu D. V. S., Sen R., Govindraj A. and Rao C. N. R., *Chem. Phys. Lett.*, **319** (2000) 296.
[23] Eswaramoorthy M., Sen R. and Rao C. N. R., *Chem. Phys. Lett.*, **304** (1999) 207.
[24] Haddon R. C., *Nature*, **378** (1995) 249.
[25] Withers A. C., Kohn S., Brooker R. and Wood B., *Geochim. Cosmochim. Acta*, **64** (2000) 1051.
[26] Romanenko A. I., Okotrub A. V., Anikeeva O. B., Bulusheva L. G., Yudanov N. F., Dong C. and Ni Y., arXiv:cond-mat/0110313.
[27] Walther J. H., Jaffe R., Halicioglu T. and Koumoutsakos P., *J. Phys. Chem. B*, **105** (2001) 9980.
[28] Bekyarova E., Hanzawa Y., Kaneko K., Albero J. S., Escribano A. S., Reinoso F. R., Kasuya D., Yudasaka M. and Iijima S., *Chem. Phys. Lett.*, **366** (2002) 463.
[29] Ghosh S. and Sood A. K., unpublished.
[30] Smith M. W. *et al.*, *Comput. Chem.*, **14** (1993) 1347.
[31] Bulusheva G., Okotrub A. V., Romanov D. A. and Tomanek D., *J. Phys. Chem. A*, **102** (1998) 975.
[32] Dattagupta S., *Relaxation Phenomena in Condensed Matter Physics* (Academic Press, Orlando) 1987, p. 139.
[33] Abragam A., *The Principles of Nuclear Magnetism* (Oxford University Press, NewYork) 1961, Chapt. 10, p. 449.